Monitoring pitting gear faults using electrical current and sound emissions

Pavle Boshkoski
Institute Jožef Stefan
Jamova cesta 39,
1000 Ljubljana, Slovenia
pavle.boskoski@ijs.si

Anton Urevc
Center for tribology and technical diagnostics
Faculty for Mechanical Engineering
University of Ljubljana
Bogišičeva 8, Slovenia
aurevc@gmail.com

Abstract— **Gearboxes are ubiquitous items of equipment in industry and pitting is one of the most frequent faults. To prevent the propagation of this fault to mechanical failure, it is necessary to monitor its initiation and evolution. Most of the current fault detection methods rely on vibration signals. The main idea of our work is to determine the detection potential and sensitivity of alternative information sources, like electrical current and sound emission. Such combination of the information from different sources provides more robust and cost effective solution.**

This paper presents the results of the experimental study of pitting fault detection exploiting sound emission and electrical current in comparison to vibration. The study is carried on a motor-generator test rig with one stage gearbox.

I. INTRODUCTION

Most of the unplanned machines shutdown are caused by mechanical faults. In this manner, early fault detection, progress monitoring and prognosis are important steps in avoiding these unplanned shutdowns. Since gearboxes are one of the most common mechanical elements present, there has been done a lot of work in the field of gear fault detection.

The research diversity is mainly aimed towards using different signal processing tools for better feature extraction from the vibration and sound emission signals. In that manner one of the most commonly used techniques is envelope analysis [9]. Recently, Antoni and Randall have proposed the usage of cyclostationary analysis through the analysis of the spectrum of the squared envelope signal [10],[1].

Apart from the analysis in the pure frequency domain, the time-frequency analysis have proven also successful in the machine condition monitoring. The usage of wavelet transform [13] has shown the capabilities of signal analysis on the whole time-frequency range.

All signal processing tools are mainly used to analyze the vibration signals [2], [11] or sound emissions [3], [12] as a information source for pitting faults. Additionally oil debris analysis has been used to detect wear particles [8]. There are very few results presenting the possibility of using electrical current as an information source for fault detection outside the motor itself [6], [16].

In most of the cases results are obtained by observing the signal's signature obtained from seeded faults [4]. There are some examples where multiple sources have been used [14]. In both cases, seeded and natural fault progression, vibration signals alone or a combination of vibration with oil or sound emission have been used.

Our main goal is to determine the fault detection capability using a combination of vibration, sound emission and electrical current. In that manner we are testing the detectability and sensitivity of each of these three sources in monitoring of natural progressing gear pitting fault.

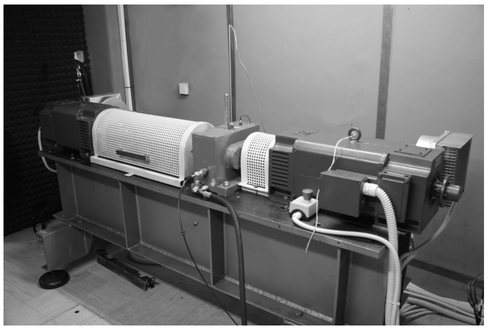

Fig. 1. The test bed

II. EXPERIMENTAL SET-UP

The signals used for our analysis are collected from an experimental test bed which consists of a motor-generator pair with a single stage gearbox (Fig. 1). The motor is a standard DC motor powered through a Simoreg DC drive. A generator has been used as a break. The generated power has been fed back in the system, thus achieving the breaking force.

Vibration signals have been gathered on 8 points: motor output shaft (Z axis), gearbox input shaft (X, Y and Z axis), gearbox housing (X, Y and Z axis) and gearbox output shaft (Z axis). All signals are gathered using Brüel & Kjær. The vibration signals were sampled with 80 kHz. Sound emission was recorder above the gearbox. The microphone was placed within a isolating tube pointing downwards. The tube converts the microphone to a pointed microphone, thus isolating the sound recording from any sound that might be emitted from the surrounding environment.

Gear ratio was 24:16, on motor vs. generator respectively. Roller bearings were used on both gearbox shafts.

III. SINGAL ANALYSIS

A. Signal model

For a meshing gear pair, that is operating under certain load, the teeth deformations occur. This deformations are dependent on the load and number of teeth in contact. The vibration signal generated from this process has spectral components at GMF [1] and its harmonics. Amplitudes of these components are directly dependent on the load amplitude. For the first M harmonics GMF ($f_{gm} = f_g N$) the signal is defined as:

$$x_1(t) = \sum_{m=1}^{M} A(F)_m cos(2\pi t f_{gm} m + \phi_m) \tag{1}$$

where $A(F)_m$ is the amplitude of the mth harmonics of the GMF, that is dependent on the load F, the number of teeth N, meshing frequency f_m, the shaft rotational frequency f_g and the phase ϕ_m of the mth harmonic of the GMF.

The instantaneous frequency of the shaft $f_g(t)$, the vibration signal is rearrange as a function of the angle $\theta_g(t)$. The equation (1) is transformed as:

$$x_1(t) = \sum_{m=1}^{M} A(F)_m cos(mN\theta_g(t) + \phi_m) \tag{2}$$

where $\theta_g(t)$ is the shaft position at the moment t.

Taking in account the geometrical faults of the teeth (manufacturing errors and non-equal finishing), we obtain additional amplification of the amplitudes of GMF and its harmonics:

$$x_1(t) = \sum_{m=1}^{M} (A(F)_m + E_m) cos(mN\theta_g(t) + \phi_m), \tag{3}$$

where E_m is the load of the mth harmonic of the GMF.

The load variation, that is periodical with the angle of the shaft $\theta_g(t)$, generates amplitude modulation of the signal.

The function of the amplitude modulation can be written as:

$$\alpha(\theta_g(t)) = \sum_{k=1}^{K} a_k cos(k\theta_g(t) + \kappa_k) \tag{4}$$

where a_k and κ_k, are the amplitude and phase of kth harmonic of the shaft rotation respectively.

The modulated signal can be written as:

$$x_1(t) = \sum_{m=1}^{M} (A(F)_m [1 + \alpha(\theta_g(t))] + E_m) \times cos(mN\theta_g(t) + \phi_m) \tag{5}$$

The frequency modulation of the signal, which occurs due to the variation of the rotational speed, is approximated with phase modulation. The function of the phase modulation is writtens as (4):

$$\beta(\theta_g(t)) = \sum_{k=1}^{K} b_k cos(k\theta_g(t) + \chi_k) \tag{6}$$

[1]GMF gear mesh frequency

where b_k and χ_k, are the frequency modulation of the kth harmonic of the GMF and phase modulation of the kth harmonic of the GMF respectively.

The frequency modulated signals is:

$$x_1(t) = \sum_{m=1}^{M} (A(F)_m [1 + \alpha(\theta_g(t)) + E_m] \times cos(mN(\theta_g(t) + \beta(\theta_g(t)) + \phi_m) \tag{7}$$

The sum of the influences, described with (7), represents the first part of the signal $x_1(t)$. The second part of the signal $x_2(t)$ is generated by the components, whose occurrence is not deterministic. Those components are due to errors in manufacturing, and additional impulses which are produce by different localized errors on the teeth. Amplitudes of those vibrations are not dependent on the load or rotational speed. They can be described as Kth harmonics of the shaft rotational frequency:

$$x_2(t) = \sum_{k=0}^{K} D_k cos(k\theta_g(t) + \xi_k) \tag{8}$$

where $D(k)$ is the amplitude of the kth harmonic of the GMF and ξ_k is the phase of the kth harmonic of the GMF.

Now we can write the vibration signal, that is generated from the meshing teeth as:

$$\begin{aligned} x(t) = & \sum_{m=1}^{M} [(A(F)_m [1 + \alpha(\theta_g(t))] + E_m) \times \\ & cos(mN(\theta_g(t) + \beta(\theta_g(t))) + \phi_m)] \\ & + \sum_{k=0}^{K} D_k cos(k\theta_g(t) + \xi_k). \end{aligned} \tag{9}$$

This mathematical vibration model is influenced by a lot of factors, which are generating far more complex signal. Different faults are represented as amplitude modulation $\alpha(\theta_g(t))$ or frequency modulation $\beta(\theta_g(t))$ of the original signal. These amplitude and frequency modulations occur as a sidebands of the GMF and its harmonics, i.e. $m \cdot f_u \pm k \cdot f_g$. With envelope analysis, i.e. with the analysis of the sidebands of the GMF and its harmonics $m \cdot f_u$, we obtain a lot of information about the nature of the fault.

B. Envelope analysis

The spectrum of the envelope signal is obtained on basis of the Hilbert transform. The envelope of the signal $x(t)$ is obtained by the amplitude of the analytical signal. The analytical signal $x_a(t)$ is a complex signal whose real part is the original signal $x(t)$, and the imaginary part is the Hilbert transform of the original signal $x(t)$ (10).

$$x_a(t) = x(t) + iH[x(t)] = a(t)e^{i\phi(t)}. \tag{10}$$

where $H[x(t)]$ is the Hilbert transform of the signal $x(t)$:

$$H[x(t)] = \frac{1}{2\pi} \int_{-\infty}^{+\infty} \frac{x(t)}{t - \tau} d\tau. \tag{11}$$

Fourier transform of the analytical signal $x_a(t)$ is:

$$X_a(t)(f) = X(f) + jH[X(t)] = \begin{cases} 2X(t) & \text{for } f > 0, \\ X(t) & \text{for } f = 0, \\ 0 & \text{for } f < 0. \end{cases} \tag{12}$$

This shows that the analytical signal has specter only in the positive frequency range. This characteristics can be used for the calculation of the analytical signal [5].
By calculating the amplitude of the analytical signal (10)

$$a(t) = \sqrt{x^2(t) + H^2[x(t)]} \tag{13}$$

we obtain the envelope of the signal.

It was shown by Ho and Randall [5] that by not doing the square root of the amplitude, thus obtaining the squared envelope, we may obtain better results. This square envelope is used when the SNR[2] is relatively low.

C. Wavelet packet decomposition

A wavelet packet function $\omega^m_{j,k}(t)$ is defined as [7]

$$\omega^m_{j,k}(t) = 2^{j/2}\omega^m(2^j t - k) \tag{14}$$

where j and k are are the scaling (frequency localization) parameter and the translation (time localization) parameter, respectively; $m = 0, 1, \ldots$ is the oscillation parameter; and $\omega^m(t)$ without any subscripts should be considered as $\omega^m_{j,k}(t)$ with $j = k = 0$.

The first two wavelet packet functions $(m = 0, 1, j = k = 0)$ are also called the scaling function $\phi(t)$ and the mother wavelet $\psi(t)$, as shown below:

$$\begin{aligned} \omega^0(t) &= \phi(t) \\ \omega^1(t) &= \psi(t) \end{aligned} \tag{15}$$

The other wavelet packet functions for $m = 2, 3, \ldots$, are defined through the following recursive relations:

$$\begin{aligned} \omega^{2m}(t) &= \sum_k h(k)\omega^m_{1,k}(t) \\ \omega^{2m+1}(t) &= \sum_k (-1)^k h(-k+1)\omega^m_{1,k}(t) \end{aligned} \tag{16}$$

Therefore, we have:

$$\begin{aligned} \omega^{2m}(t) &= \sqrt{2}\sum_k h(k)\omega^m(2t - k) \\ \omega^{2m+1}(t) &= \sqrt{2}\sum_k (-1)^k h(-k+1)\omega^m(2t - k) \end{aligned} \tag{17}$$

where $h(k) = \frac{1}{\sqrt{2}}\langle\phi(t), \phi(2t - k)\rangle$. Where $\langle\cdot,\cdot\rangle$ stands for inner product.

For each $m = 0, 1, \ldots$, the function cluster

$$\left\{2^{j/2}\omega^m(2^j t - k) | j, k = \ldots, -2, -1, 0, 1, 2, \ldots\right\}$$

constitutes the normal orthogonal basis. In other words for a certain m' the wavelet packet functions $2^{j/2}\omega^{m'}(2^j t - k)$ are located in a specific frequency band. All the frequency bands constitute a normal orthogonal basis in the time-frequency subspace. The time-frequency space V_m can be formed by the combination of $\omega^{2m}_{j,k}(t)|j, k = \ldots, -1, 0, 1, \ldots$ and $\omega^{2m+1}_{j,k}(t)|j, k = \ldots, -1, 0, 1, \ldots$. Wavelet packet coefficients of a signal $x(t)$ are embedded in the inner product of the signal with every wavelet packet function, denoted by $P^m_j(k)|k = \ldots, -1, 0, 1, \ldots$ and given as:

$$P^m_j(k) = \langle x, \omega^m_{j,k}\rangle = \int_{-\infty}^{\infty} x(t)\omega^m_{j,k}(t)dt \tag{18}$$

where $P^m_j(k)$ denotes the m^{th} set of wavelet packet decomposition coefficients at the jth scale parameter and k is the translation parameter. All frequency components and their occurring times are reflected in $P^m_j(k)$ through change of m, j, k. Each $P^m_j(k)$ coefficient measures a specific sub-band frequency content, controlled by the scaling parameter j and the oscillation parameter m. The essential function of WPT is the filtering operation through $h(k)$ and $g(k)$.

By computing the full wavelet packet decomposition on a data vector $x(t)$, for the jth level of decomposition, we have 2^j sets of sub-band coefficients of length $N/2^j$. The total number of such sets located at the first level to the jth level inclusive is $(2^{j+1} - 2)$. The order of these sets at the jth level is $m = 1, 2, \ldots, 2^j$. Then, each set of coefficients can be viewed as a node in a binary wavelet packet decomposition tree. Wavelet packet coefficients, $P^m_j(k)|k = 1, 2, \ldots, N/2^j$, correspond to node (j, m). From each node (j, m), we obtain a reconstructed signal $P^1_0(k)|k = 1, 2, \ldots, N$ by setting the coefficients of all other nodes at the jth level to zero. Reconstructed signals $P^1_0(k)|k = 1, 2, \ldots, N$ obtained from $P^m_j(k)|k = 1, 2, \ldots, N/2^j$ reflect the change of the signal with time in the frequency range of $[(m-1)F_s/2^{j+1}, m \cdot F_s/2^{j+1}]$, where F_s is the sampling frequency. As a result, there are m sets of reconstructed signals that contain the necessary information for detection of characteristic frequencies of faults in different frequency ranges.

IV. RESULTS

The test run was done with a constant torque of 82.5 Nm and constant speed of 990rpm. This speed of 990rpm generates GMF $f_{gm} = 396Hz$, rotational speed of input shaft $f_i = 16.5Hz$, and rotational speed of output shaft $f_o = 24.75Hz$.

During the experiment run vibration and electrical current signals were sampled with 80kHz and the sound emissions were sampled with 44kHz. The signals were sampled every 10 min. The duration of the sampled signal was 5 seconds, which yields 400 000 samples per signal for vibration and electrical current, and 220 000 samples for sound emission signal.

In order to speed up the experiment, the contact surface between the gears was decreased to $1/3$ of the original surface. In this manner the pressure excreted on the gear teeth was bigger thus generating the fault faster. This displacement is shown on Fig. 2(a).

The test started with a brand new gears. After a 1000 hours run the gears were swapped with a heavily pitted gears, shown on Fig. 2(b), and the experiment was resumed for

[2]SNR signal to noise ratio

another 200 hours. In the new set of gears, the gear mounted on the output shaft had more damage. The gear state after 1000 hours is shown on Fig. 2(a).

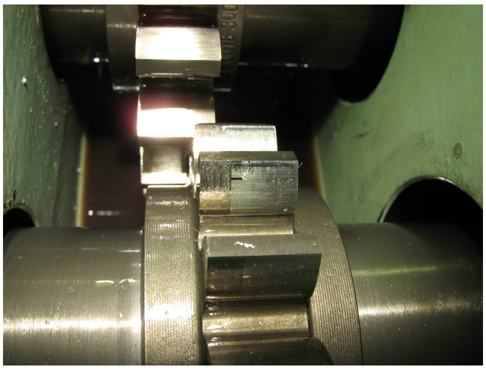

(a) Scuffing

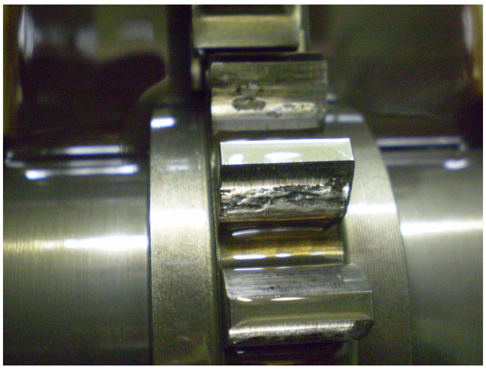

(b) Strong pitting

Fig. 2. Two different gear damage

A. Vibration analysis

According to the vibration signal model (9) the vibration signals were analyzed with envelope analysis method. Fig. 3 shows the trends of a particular components of the amplitude spectra. It can be noticed that the spectra show some increase in the signals around 300 hrs. After this initial increase the vibration levels decrease. The increase trend reappears after 500 hours, from which point it show steady increase.

This non-monotonic behavior of the vibration's trend is due to the effect of self polishing i.e. after an initial fault evolved (after 300 hrs) the natural wear of the gears polished the surface and the vibration decreased. Although there is a decrease, it can be seen in the GMF graph in Fig. 3 that the level after 300 hrs is bigger then the initial level of vibrations.

In order to compare the increase of vibration levels of this initial fault (scuffing) with a heavy pitting fault, the gears were swapped with heavily pitted gears. The compared trends are shown on Fig. 4, i.e. the heavy pitted gear signals are added to the original graphs Fig. 3, thus covering the time from 650hrs onwards. There is a big increase in the vibration levels. Similarly like the initial run, the vibration trends show non-monotonic behavior. After initial 50 hrs the vibration levels decreased. This initial time might be considered like a run-in time. After the run-in time, the non-monotonic trend continues, however during the whole time the level of vibration is hugely bigger then the initial state.

Trends presented on Fig. 4 are conforming with the fact that the output gear has bigger damage then the input gear. Throughout the run with the heavily pitted gears the f_o component is several times bigger then the f_i component.

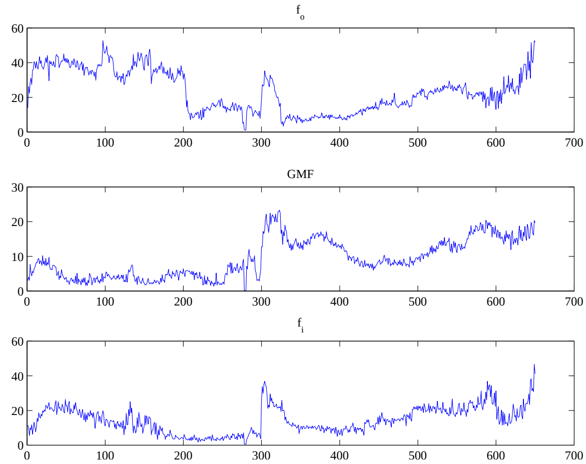

Fig. 3. Vibration trends

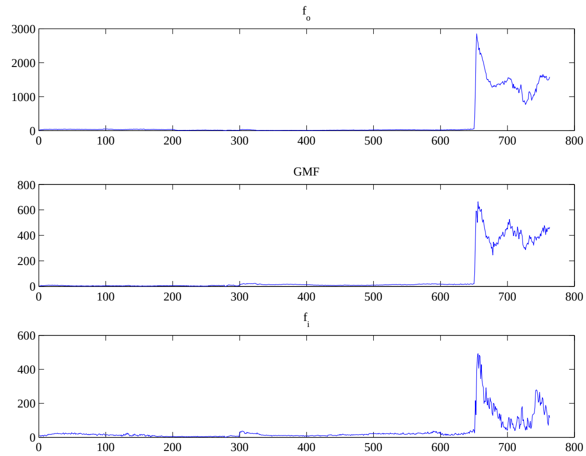

Fig. 4. Vibration trends with added damaged gear

B. Sound emission

The sound emissions were gathered using a microphone positioned directly above the gearbox. The microphone was shielded so it was able to pickup sounds only from the surface directly below. In this manner we tried to isolate any possible environmental sounds that might interfear with the measurements.

Similarly like the vibration signals, the sound emission was analyzed using the envelope method Eq. (13). The trend of the GMF is shown on Fig. 5. Unlike the vibration signals the sound emission are showing constant trends throughout the experiment. After approx. 400 hrs. the first increase in the levels of GMF occurs. From this moment onwards the increasing trend is steady.

The same observation applies and for the case of heavily pitted gears, shown on Fig. 6, i.e. the signals covering the time from 650hrs. After the initial run-in (around 650-th hour) the sound emissions decreased a level and stayed constant. The level of sound GMF amplitude in this case is significantly bigger then the same level during the run of gears with scuffing fault (0-650 hrs.).

Similarly like the vibration signal, the trends for the heavily pitted gears (Fig. 6), are showing bigger damage of the output gear then the damage on the input gear. The amplitudes of the f_o components are almost 2 times bigger then the components of the f_i frequency.

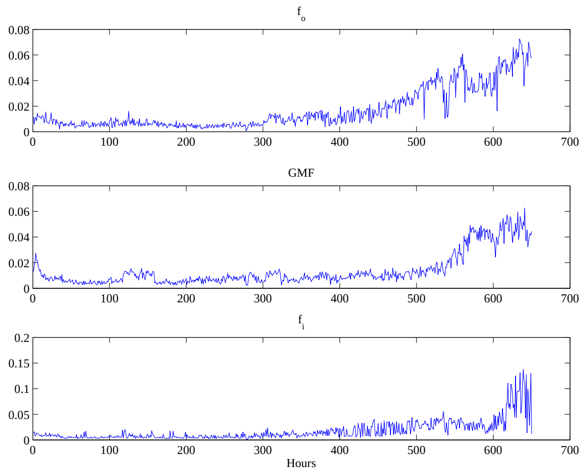

Fig. 5. Sound emission trends

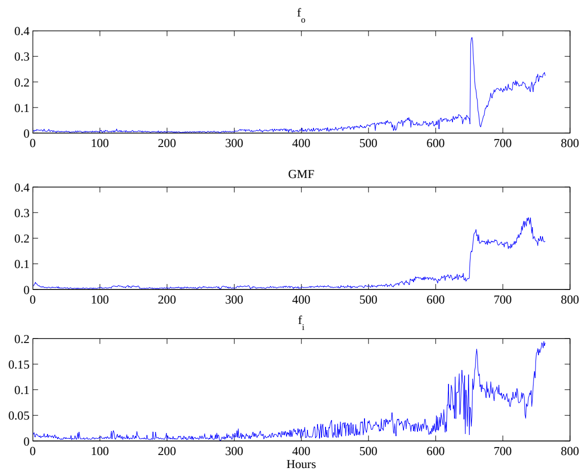

Fig. 6. Sound emission trends with added damaged gear

C. Electrical current

The supply to the DC motor is obtained by rectifying 3 phase AC power supply. This convertion generates a waveform as shown on Fig. 7. This signal has dominant frequency components at 300Hz, which is the supply line frequency. As shown in the [15] the torsional torque changes are reflected as a side bands of the supply line frequency of the electrical machines. Due to this effect the envelope analysis does not yields good results.

We have applied wavelet packet decomposition on the electrical current signal. The signal was decomposed using *discrete Meyer wavelet* on 13 levels which produced a wavelet leaves covering 4.88 Hz of bandwidth.

We have monitored the GMF and shaft frequencies side-bands of the line frequency (300Hz), i.e

$$\begin{aligned} &n300 \pm GMF \\ &n300 \pm f_i \\ &n300 \pm f_o \end{aligned} \quad (19)$$

The trends of the signal during the run in the first 650 hours is shown in Fig. 8. It can be noticed that the sidebands of the rotational speed of the input and output shafts don't show any trends. On the other hand, the low sideband GMF trend, shown on the middle graph on Fig. 8, show increase in its amplitude after 500 hours of operation. This moment is comparable to the results obtained with the vibration and sound emission signals.

Observing the same trends but for the period when the machine was running with a heavily pitted gears (Fig. 9), it is becoming evident the increase of the GMF sideband component. This increase is approximately twice in the amplitude. Additionally the side band of the f_o, the output shaft shows increase, pointing towards damage of the output gear. This results is again conforming with the results obtained from analysis of the previous two signals.

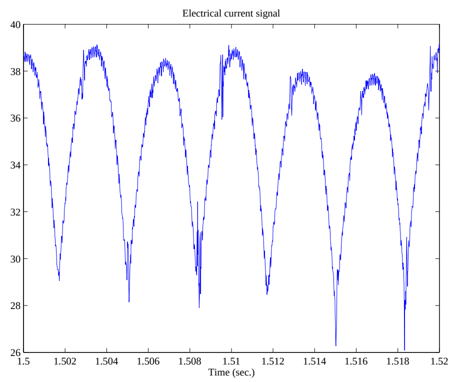

Fig. 7. Electrical signal

D. Compared sensitivity

The compared signal trends are shown on Fig. 10. First two graphs are showing trends of the input (red) and output (blue) shaft frequency components. The third graph shows the trends of the sideband of 1296Hz (900Hz + GMF) of the electrical current signal. Even when the faults are minor, like in this case scuffing fault, the detection is possible by monitoring of any of the three signals. From all three the electrical current has less sensitivity but even with that sensitivity it can be considered as a reliable source for

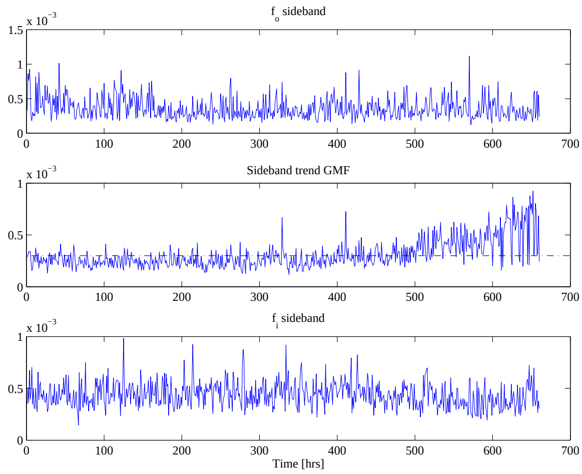

Fig. 8. Electrical current trends

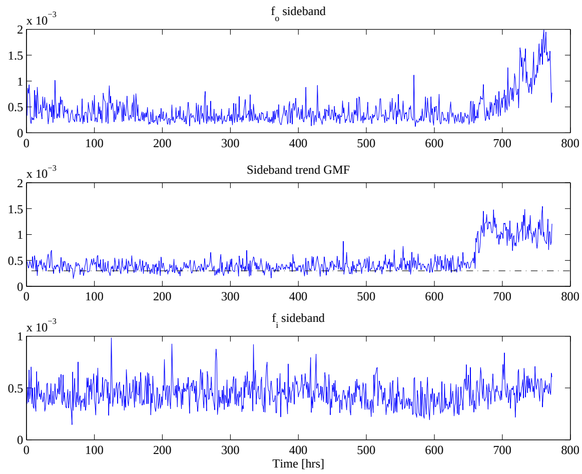

Fig. 9. Electrical current trends with added bad gears

pitting detection. Sound emission signals are able to detect the initial fault generation earliest. In comparison the sound emission show steady increase in amplitude levels of a certain frequency components, unlike the vibration signal where the amplitude levels are fluctuating due to the self polishing.

V. CONCLUSION

By comparing the results obtained with this experiment, it is shown that in both cases, scuffing and heavy pitting, sound emissions and electrical current may be used for fault detection. By adding multiple sources to the detection system we are able to increase the accuracy of the fault detection. This increase in the accuracy leads towards increase of the reliability of the fault detection system.

In comparison with the vibration signals, sound emissions and electrical current can be acquired by far cheaper equipment, as it was done in this work.

This leads to a conclusion that a reliable and cheap fault detection system may be build using combination of any of three examined sources, or all of them like in our case.

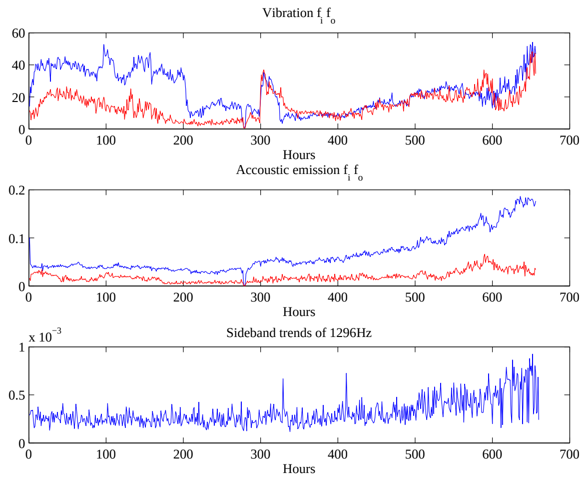

Fig. 10. Vibration trends

REFERENCES

[1] J. Antoni. Cyclic spectral analysis in practice. *Mechanical Systems and Signal Processing*, 21:597 – 630, 2007.

[2] N. Baydar and A. Ball. Detection of gear failures via vibration and acoustic signals using wavelet transform. *Mechanical Systems and Signal Processing*, 17:787 – 804, 2003.

[3] U. Benko, J. Petrovčić, D. Juričić, J. Tavčar, and J. Rejec. An approach to fault diagnosis of a vacuum cleaner motors based on sound analysis. *Mechanical Systems and Signal Processing*, 19:427 – 445, 2005.

[4] X. Fan and M. J. Zuo. Gearbox fault detection using hilbert and wavelet packet transform. *Mechanical Systems and Signal Processing*, 20:966 – 982, 2006.

[5] D. Ho and R. B. Randall. Optimisation of bearing diagnostic techniques using simulated and actual bearing fault signals. *Mechanical Systems and Signal Processing*, 14:763–788, 2000.

[6] C. Kar and A. R. Mohanty. Monitoring gear vibrations through motor current signature analysis and wavelet transform. *Mechanical Systems and Signal Processing*, 20:158–187, 2006.

[7] S. Mallat. *A wavelet tour of signal processing, Second edition*. Academic Press, 1999.

[8] Z. Peng and N. Kessissoglou. An integrated approach to fault diagnosis of machinery using wear debris and vibration analysis. *Wear*, 255:1221–1232, 2003.

[9] R. B. Randall. *Frequency analyses*. Brüel and Kjær, 1987.

[10] R. B. Randall, J. Antoni, and S. Chobsaard. The relationship between spectral correlation and envelope analysis in the diagnostics of bearing faults and other cyclostationary machine signals. *Mechanical Systems and Signal Processing*, 15:945 – 962, 2001.

[11] N. Sawalhi, R.B. Randall, and H. Endo. The enhancement of fault detection and diagnosis in rolling element bearings using minimum entropy deconvolution combined with spectral kurtosis. *Mechanical Systems and Signal Processing*, 21:2616–2633, 2007.

[12] J.Z. Sikorska, P.J. Kelly, and J. Pan. Development of an ae data management and analysis system. *Mechanical Systems and Signal Processing*, 20:2321–2339, 2006.

[13] Cary Smith, Cajetan M. Akujuobi, Phil Hamory, and Kurt Kloesel. An approach to vibration analysis using wavelets in an application of aircraft health monitoring. *Mechanical Systems and Signal Processing*, 21:1255–1272, 2007.

[14] C.K. Tan, P. Irving, and D. Mba. A comparative experimental study on the diagnostic and prognostic capabilities of acoustics emission, vibration and spectrometric oil analysis for spur gears. *Mechanical Systems and Signal Processing*, 21(1):208–233, 2007.

[15] R. Yacamini, K. S. Smith, and L. Ran. Monitoring torsional vibrations of electro-mechanical systems using stator currents. *Journal of Vibration and Acoustics, Transactions of ASME*, 120:72–79, 1998.

[16] J. Zarei and J. Poshtan. Bearing fault detection using wavelet packet transform of induction motor stator current. *Tribology International*, 40:763–769, 2007.